The Dynamics of Greenland's Glacial Fjords and Their Role in Climate

Fiamma Straneo and Claudia Cenedese

Woods Hole Oceanographic Institution, Woods Hole, Massachusetts 02543;
email: fstraneo@whoi.edu, ccenedese@whoi.edu

Annu. Rev. Mar. Sci. 2015. 7:89–112

First published online as a Review in Advance on August 13, 2014

The *Annual Review of Marine Science* is online at marine.annualreviews.org

This article's doi:
10.1146/annurev-marine-010213-135133

Keywords

glacial fjords, Greenland, submarine melting

Abstract

Rapid mass loss from the Greenland Ice Sheet has sparked interest in its glacial fjords for two main reasons: Increased submarine melting of glaciers terminating in fjords is a plausible trigger for glacier retreat, and the anomalous freshwater discharged from Greenland is transformed by fjord processes before being released into the large-scale ocean. Knowledge of the fjords' dynamics is thus key to understanding ice sheet variability and its impact on climate. Although Greenland's fjords share some commonalities with other fjords, their deep sills and deeply grounded glaciers, the presence of Atlantic and Polar Waters on the continental shelves outside the fjords' mouths, and the seasonal discharge at depth of large amounts of surface melt make them unique systems that do not fit existing paradigms. Major gaps in understanding include the interaction of the buoyancy-driven circulation (forced by the glacier) and shelf-driven circulation, and the dynamics in the near-ice zone. These must be addressed before appropriate forcing conditions can be supplied to ice sheet and ocean/climate models.

1. INTRODUCTION

Submarine melting: melting of the portion of a glacier front that is immersed in water

Glacier front: the terminus of a marine-terminating glacier at the head of a fjord

Mass loss from the Greenland Ice Sheet (GrIS) quadrupled over the past two decades owing to increased surface melt and the widespread retreat and speedup of marine-terminating glaciers (van den Broeke et al. 2009, Shepherd et al. 2012, Enderlin et al. 2014). This loss resulted in a 7.5-mm rise in global sea level from 1992 to 2011, making Greenland alone responsible for one-quarter of the present rate of sea level rise (Church et al. 2011). Greenland's ice loss is also leading to an anomalous freshwater input into the North Atlantic, contributing 3,200 km^3 of freshwater since 1995, i.e., approximately one-third of the volume of the Great Salinity Anomaly of the 1970s (Bamber et al. 2012)—a freshwater anomaly of Arctic origin that disrupted convection in the Labrador Sea (Lazier 1980). The implication is that the GrIS discharge is now important for the freshwater budget of the North Atlantic, and if it persists, it is likely to have an impact on both the regional ocean (including the marine ecosystem) and the global ocean (through the Atlantic Meridional Overturning Circulation).

These large changes have sparked interest in Greenland's glacial fjords—the links between the ice sheet and the large-scale ocean, hereafter generally referred to simply as fjords—for two main reasons. First, consistent with rising ocean and air temperatures, it is plausible that a sizable portion of the recent mass loss (i.e., the portion resulting from glacier retreat) was triggered by increased submarine melting of the glaciers' margins, which are located at the heads of Greenland's fjords (for reviews, see Vieli & Nick 2011, Straneo & Heimbach 2013). Second, most of the freshwater discharged from Greenland transits through the fjords, where it can be transformed by fjord processes before reaching the large-scale ocean. Knowledge of the fjords' dynamics and processes is thus key to estimating glacier melt rates, and their controls, and to determining where and when the freshwater enters the ocean. Ultimately, an understanding of the fjords' dynamics is necessary to explain changes in Greenland, elucidate their impact on the climate system, and predict future changes [see review by Straneo et al. (2013)].

Several unique characteristics of Greenland's fjords set them apart from other fjords and raise questions about the applicability of existing fjord theories. First, Greenland's large fjords, which are often associated with the largest glaciers, have sills that are several hundred meters deep. The theories for hydraulically controlled flows (e.g., Farmer & Freeland 1983) are therefore not readily applicable in Greenland. Second, Greenland's continental shelves are characterized by a confluence of two water masses: light waters of Arctic origin and relatively dense waters of Atlantic origin. The deep sills allow both waters to enter the fjords, resulting in a strongly stratified water column before the additional freshwater is discharged into the fjord. This is in contrast to the assumption made by most fjord theories that a single water mass from the coastal region flows into the fjord. Finally, surface melting of the GrIS occurs all around its margins, resulting in a large, seasonal freshwater discharge at the bases of glaciers, hundreds of meters below sea level. The release of large volumes of surface melt at depth contributes to some major differences between Greenland's glacier-ocean interactions and those from other regions, including Antarctica, where surface melt may be limited and/or the glaciers are grounded closer to the surface.

The aim of this review is to summarize what we know about the dynamics of Greenland's fjords and what this implies for submarine melting and freshwater export into the ocean. These are not the only reasons to study the fjords, however. The fjords contain records of past ice sheet and glacier variability (e.g., Andresen et al. 2012); are regions of complex sedimentation patterns that, in turn, may be affecting glacier behavior (for a review, see Syvitski 1989); and sustain large, complex marine ecosystems and support local populations that depend on the fjords for hunting, fishing, and traveling (Born & Böcher 2001). This review builds on existing reviews of fjord dynamics (e.g., Farmer & Freeland 1983, Cottier et al. 2010, Inall & Gillibrand 2010, Stigebrandt

2012) and does not attempt to summarize all possible fjord processes. Instead it focuses on what we believe are the dominant and unique dynamics of Greenland's fjords. Finally, this review focuses primarily on Greenland's large fjords, which are associated with the largest glaciers and are the largest contributors to the recent changes; for example, 15 of Greenland's glaciers account for more than 50% of the ice discharge (Enderlin et al. 2014). The large glacial fjords have also been the focus of recent observational efforts and thus are the systems we know the most about.

This review is structured as follows. First, we summarize some basic characteristics of Greenland's fjords (Section 2). Next, we discuss the fjord dynamics within three dynamically distinct regions: the ice-ocean boundary layer (Section 3), the plume region (Section 3), and the larger fjord system (Section 4). The implications for submarine melting and freshwater export are discussed in Sections 5 and 6, respectively. At the end, we provide a summary and a future outlook.

2. CHARACTERISTICS OF GREENLAND'S GLACIERS AND GLACIAL FJORDS

Fjords are narrow, deep inlets carved by glaciers, often characterized by one or more sills. Glacial fjords are fjords with a marine-terminating (tidewater) glacier. In Greenland, glacial fjords connect the GrIS to the North Atlantic subpolar gyre, Baffin Bay, the Nordic Seas, and the Arctic Ocean (**Figure 1*a***). They are long (50–100 km), narrow (5–10 km), and deep (hundreds of meters). Sill depths vary considerably but are typically hundreds of meters for the large fjords (**Figure 1*b*,*c***). Properties of the water inside the fjords (ambient water) resemble those on the nearby continental shelves, where cold, relatively fresh water of Arctic origin [Polar Water (PW)] carried by the East and West Greenland Currents (Myers et al. 2007, Sutherland & Pickart 2008) overlies warm, salty water of Atlantic origin [Atlantic Water (AW)] flowing in different branches around the basins (Holland et al. 2008, Rignot et al. 2010, Straneo et al. 2010, Christoffersen et al. 2011). Temperature and salinity profiles from five of Greenland's largest glacier/fjord systems are shown in **Figure 1*b*,*c***. The properties of the AW and PW vary around Greenland depending on the distance from their source regions (Straneo et al. 2012) (e.g., **Figure 1*b*,*c***).

Obtaining data from Greenland's fjords is difficult and costly because of the fjords' remoteness and the challenges posed by calving glaciers and icebergs. Where surveys exist, they show that the large fjords are filled with the same AW and PW as are found on the nearby shelves (**Figure 2*a–c***). In general, along-fjord variations tend to dominate over across-fjord variations, consistent with the fact that many fjords are too narrow for the circulation to be influenced by the Earth's rotation (e.g., Straneo et al. 2010, Johnson et al. 2011, Sutherland et al. 2014). Of the five fjords included in **Figure 1**, one would expect to see across-fjord gradients in properties, owing to the Earth's rotation, for the fjords of the 79 North Glacier (79NG) and Petermann Glacier (PG), whose mean widths are ∼20 km, but much less so for those associated with Helheim Glacier (HG, which discharges into a fjord with a different name: Sermilik Fjord), Kangerdlugssuaq Glacier (KG), and Jakobshavn Isbræ (JI), whose mean widths are ∼4–8 km. (We hereafter use the abbreviations 79NG, PG, HG, KG, and JI to refer to both the glaciers and the associated fjords.) Velocity and property data from HG and KG have confirmed that most of the variability occurs in the along-fjord direction except near their mouths, which in both cases are wide enough that rotational effects can result in across-fjord density and velocity gradients (Straneo et al. 2010, Sutherland et al. 2014). Hydrographic data from PG show isopycnals sloping across the fjord, consistent with the expected influence of rotation (Johnson et al. 2011).

The characteristics of Greenland's tidewater glaciers vary. At one end are fast-moving glaciers with mostly vertical glacier fronts (e.g., JI, which can flow at 17 km/y; Joughin et al. 2014), for which the mass balance is controlled mainly by the periodic breakoff of icebergs (calving). The

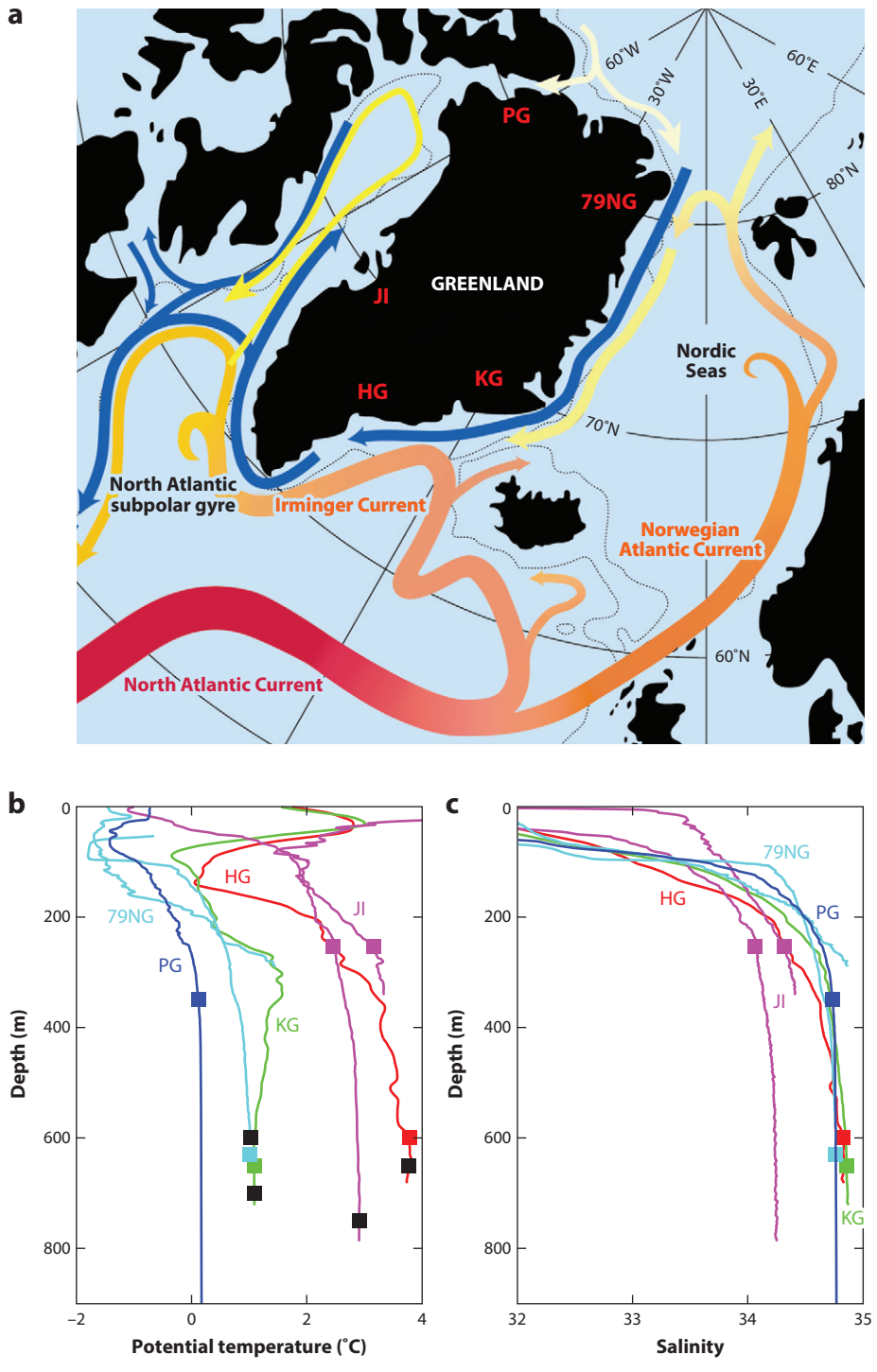

Figure 1

Ocean circulation around Greenland and water properties in five large glacial fjords. (*a*) Schematic circulation of warm, salty Atlantic Water (*red to yellow*) and cold, fresh Polar Water (*blue*) around Greenland. (*b*,*c*) Profiles of potential temperature (panel *b*) and salinity (panel *c*) in the vicinity of the mouths of five of Greenland's largest glacial fjords, corresponding to Helheim Glacier (HG), Jakobshavn Isbræ (JI), Kangerdlugssuaq Glacier (KG), the 79 North Glacier (79NG), and Petermann Glacier (PG). Panel *a* shows the glacier locations. In both sets of profiles, the colored squares indicate the sill depths of the fjords; in the temperature profiles, the black squares additionally indicate the grounding line depths. The Atlantic Water and Polar Water layering in the fjords is evident from the temperature profiles. Figure modified from Straneo et al. (2012).

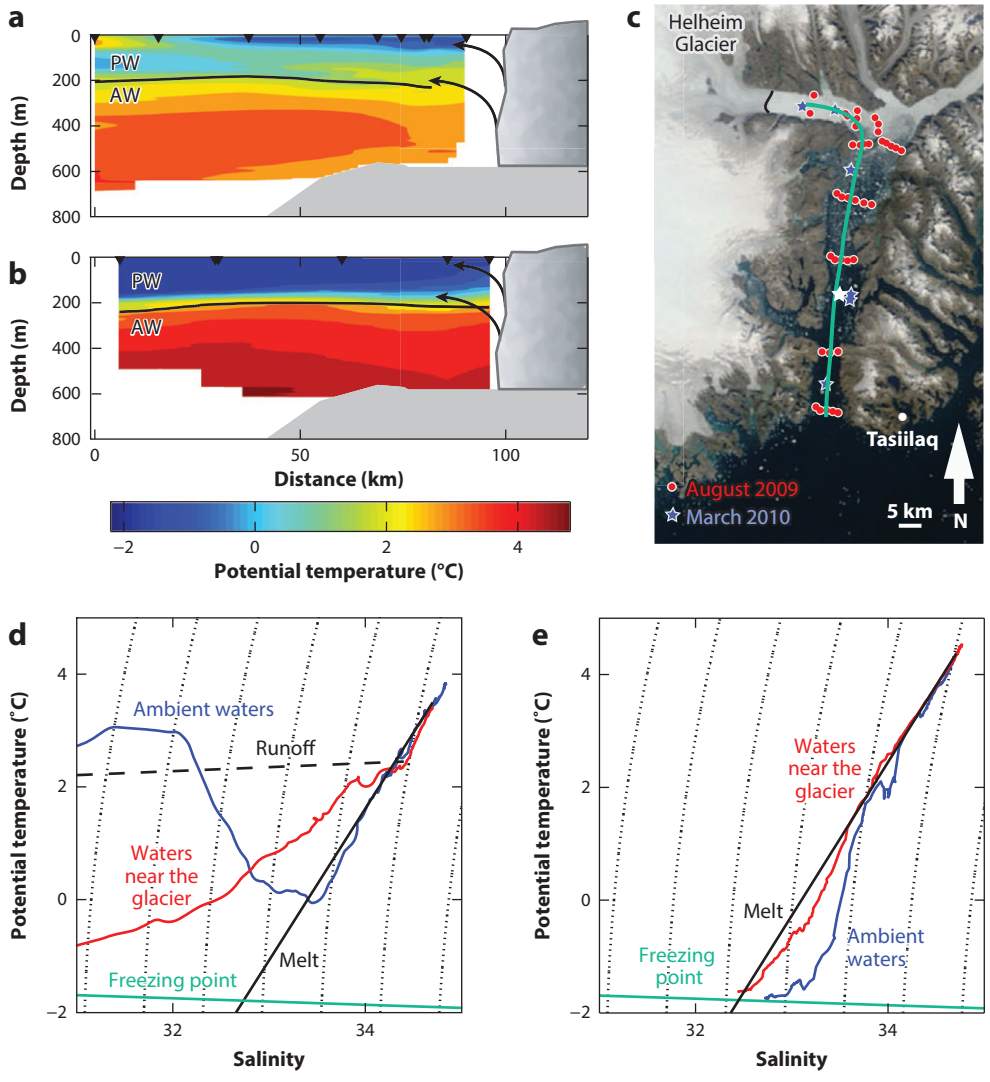

Figure 2

Distribution of water properties in Sermilik Fjord at the edge of Helheim Glacier. (*a*,*b*) Potential temperature from an along-fjord section in August 2009 (panel *a*) and March 2010 (panel *b*). The arrows indicate the intrusions of glacially modified waters. (*c*) Station locations (*red* and *blue symbols*) and approximate section location (*green line*) shown on a satellite image of the fjord. (The white star indicates the location of the mooring that provided the data shown in **Figure 5**; see Section 4.2.) (*d*,*e*) Potential temperature versus salinity (θ/S) plots at the mouth (*blue*) and near the glacier (*red*) for August 2009 (panel *d*) and March 2010 (panel *e*). Overlaid are the melt line (*solid black*), runoff line (*dashed black*) (see sidebar, Ice Melting in Ocean Water), freezing-point line (*solid green*), and isopycnals (*dotted curves*). These θ/S plots show the transformation of ambient waters found near the mouth into a water column containing glacially modified waters found near the glacier. In summer (panel *d*), the glacially modified water contains both submarine melt and subglacial discharge (i.e., in θ/S space, its properties are within a triangle enclosed by the melting and runoff lines; see sidebar, Ice Melting in Ocean Water). In winter (panel *e*), the θ/S properties of the glacially modified water are along the melt line, as expected from a transformation caused mostly by submarine melting. Abbreviations: AW, Atlantic Water; PW, Polar Water. Figure modified from Straneo et al. (2011).

fjords associated with these glaciers are typically clustered with icebergs and have a densely packed ice mélange near the glacier (a mixture of sea ice and icebergs that may influence glacier flow; Amundson et al. 2010). At the other extreme are glaciers with 50–100-km-long floating ice tongues (e.g., 79NG and PG). These glaciers flow at much slower speeds (e.g., 1 km/y for PG; Münchow et al. 2014), and mass balance is achieved primarily by submarine melting under the long floating ice tongue.

Subglacial discharge: the fraction of surface glacier melting that is discharged in the fjords at the bases of glaciers

Buoyant plumes: plumes forced by subglacial discharge and/or submarine melt that entrain ambient water as they rise along the glacier front

One important characteristic of Greenland's fjords is that they funnel large amounts of seasonal surface melt, which occurs around the marine margins of the ice sheet, toward the ocean. Surface melt within a glacier's catchment basin is channeled to the glacier's bed via the glacier's hydrologic network (Das et al. 2008, Chu et al. 2009) and is thought to be discharged in the fjords largely at the base of the glacier, i.e., at the grounding line depth (for a review, see Chu 2014). This freshwater, here termed subglacial discharge, is exported into the fjord either through several discrete channels or as a distributed source at the base of the glacier. Localized channels give rise to localized plumes that can at times emerge as turbid plumes at the surface near the edges of glaciers (e.g., Chu et al. 2009).

3. DYNAMICS IN THE NEAR-ICE ZONE

In describing fjord dynamics, we identify three different regions: the turbulent ice-ocean boundary layer (a few meters thick), the plume region (a few tens of meters thick), and the large fjord system (50–100 km long). Processes within the near-ice zone (which includes the boundary layer and the plume) regulate the exchange of heat and mass across the ice-ocean interface, including any phase change. The dynamics at the larger fjord scale (see Section 4), by contrast, are responsible for the supply of warm water to the vicinity of the glacier and the export of freshwater from the fjord to the continental shelf region. Observations near the glaciers' fronts are scarce, but the flow here is conceptualized as a system of rising buoyant plumes driven by submarine melting and subglacial discharge. Within a few meters of the ice, the ice-ocean boundary layer consists of a turbulent region (a few meters thick) where the turbulence is unaffected by the boundary and, closer to the ice, a viscous sublayer (a few millimeters thick) where the turbulent eddies are suppressed and molecular processes dominate the exchanges (Holland & Jenkins 1999, Jenkins et al. 2010) (**Figure 3*a***). Here, we summarize current theories for the leading-order dynamics within each region.

3.1. The Ice-Ocean Boundary Layer

At the glacier front, the interaction between the ice and the fjord water determines the heat and freshwater fluxes associated with phase changes at the interface. A correct representation of these fluxes is fundamental for a reliable estimate of the glacier melt rate. Measurements from this region are scarce, and models typically rely on a melt rate parameterization of the ice front based on a three-equation model (Hellmer & Olbers 1989, Holland & Jenkins 1999).

This model describes the thermodynamical equilibrium at the ice-ocean interface and solves the linear equation for the freezing temperature of seawater together with the equations for the conservation of heat and salinity. At the ice-ocean interface,

$$T_b = \lambda_1 S_b + \lambda_2 + \lambda_3 Z_b, \quad (1)$$

where the last term is the freezing-point temperature dependence with depth; the subscript b indicates the conditions at the ice-ocean interface; and λ_1, λ_2, and λ_3 are constants. The heat flux supplied to the glacier by the ambient fjord water, Q_a^T, must be balanced by the heat flux into the

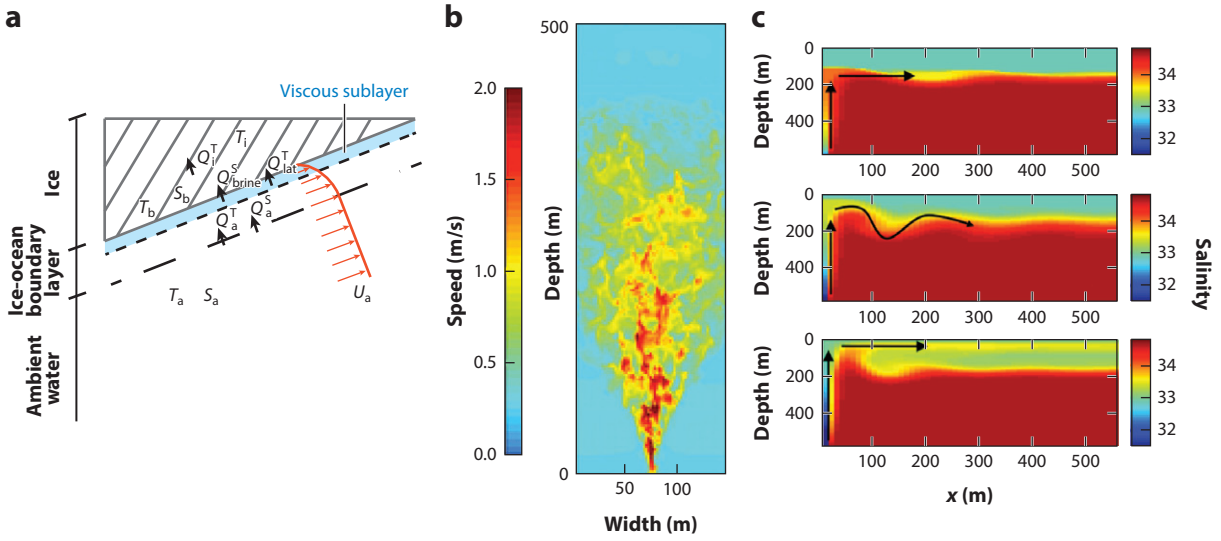

Figure 3

(*a*) Schematic representation of heat and salt fluxes at the base of an ice shelf. (*b*) Depth-width cross section of vertical velocity adjacent to the ice front in a three-dimensional simulation (using the MIT General Circulation Model) with a point source of subglacial discharge (total depth = 500 m). (*c*) Different vertical penetration depths of a buoyant plume driven by three different values of subglacial discharge. Panel *a* modified from Holland & Jenkins (1999); panel *b* modified from Xu et al. (2013); panel *c* modified from Sciascia et al. (2013).

ice, Q_i^T, and the latent heat flux associated with melting (or freezing), Q_{lat}^T:

$$Q_a^T = Q_i^T - Q_{lat}^T \tag{2}$$

where the subscripts a and i indicate conditions in the ambient water and the ice, respectively, and the superscript T indicates temperature (**Figure 3*a***; see also sidebar, Ice Melting in Ocean Water). A similar equation must be satisfied to conserve salt in the presence of the freshwater flux associated with the melting (or freezing) of ice, Q_{brine}^S:

$$Q_a^S = Q_i^S - Q_{brine}^S, \tag{3}$$

where the superscript S indicates salt (**Figure 3*a***). Because the salinity of the ice is approximately zero, we assume that the diffusive flux of salt into the ice is zero.

Equations 2 and 3 can be expressed in terms of the known ambient and ice properties (Holland & Jenkins 1999):

$$C_p \gamma_T (T_a - T_b) = \dot{m} C_i (T_b - T_i) + \dot{m} L, \tag{4}$$

$$\gamma_S (S_a - S_b) = \dot{m} (S_b - S_i), \tag{5}$$

where $\dot{m}$ is the melt rate per surface area; C_p and C_i are the specific heat capacities for seawater and ice, respectively; L is the latent heat of fusion; and γ_S and γ_T are the salinity and thermal exchange velocities, respectively, which take into account the nonlinear profiles of T and S in the boundary layer resulting from turbulence. The first term on the right-hand side of Equation 4 represents the heat flux into the ice, which has been calculated using a steady-state, one-dimensional advection-diffusion equation (Holland & Jenkins 1999).

ICE MELTING IN OCEAN WATER

Ice melting occurs in two steps: The ice is first warmed from θ_i (ice temperature) to θ_f (freezing-point potential temperature), and the latent heat is then provided for the phase transition. For submarine melting, the necessary heat is extracted from the ambient ocean waters, which are cooled as a result. The meltwater (at freezing-point temperature and zero salinity) then mixes with the ambient water, forming a mixture that is fresher than the original ambient water. When there is a single ambient water (θ_a, S_a), the properties of the meltwater/ambient water mixture can be predicted from simple heat and salt conservation principles (Gade 1979). The mixture θ/S properties fall along a straight line (melt line in **Figure 2*d*,*e***) connecting the ambient water and the effective ice properties (θ_i^*, S_i), where $S_i = 0$ and

$$\theta_i^* = \theta_f - \frac{L}{C} - \frac{C_i}{C}(\theta_f - \theta_i)$$

Erratum

is an effective ice temperature that takes into account the cooling of the water due the melting of the ice; L is the latent heat of fusion, and C_i and C are the specific heat capacities of ice and water, respectively. The slope of this line (~2.8°C per practical salinity unit) is known as the Gade slope. The fraction of meltwater by mass is

$$M_i = \frac{\theta_a - \theta}{\theta_a - \theta_i^*}.$$

If melting of the glacier front is not driven by a single ambient water mass, the meltwater fraction can still be estimated for some special cases (see Jenkins 1999). If subglacial discharge is present, then glacially modified waters can also contain a fraction of subglacial discharge (freshwater typically assumed to be at the freezing-point temperature at the local pressure). In this case, the θ/S properties of the mixture will lie between a runoff line (straight mixing line between ambient and subglacial discharge properties) and the melt line (straight line between ambient and submarine melt properties) (**Figure 2*d*,*e***). If the ambient water is composed of a single water mass, then the meltwater and subglacial discharge fractions can still be estimated (Mortensen et al. 2013); otherwise, the system is underdetermined.

A realistic estimate of the melt rate depends on a suitable choice for the exchange velocities. In the turbulent boundary layer, the heat and salt diffuse at the same rate, whereas in the viscous sublayer (**Figure 3*a***), the turbulent eddy size is reduced, such that the turbulent diffusivity diminishes and is replaced by molecular diffusivity (Mellor et al. 1986, McPhee et al. 1987, Steele et al. 1989). Therefore, in this region heat diffuses more rapidly than salt, and because the exchange velocities are parameterizing all these processes in the boundary layer, γ_S must be smaller than γ_T. Another feature of the exchange velocities is the dependence on the shear stress at the ice-ocean interface, which is parameterized in terms of a friction velocity $u_*^2 = C_D U_a^2$, where C_D is the drag coefficient and U_a is the velocity in the ambient water adjacent to the ice-ocean interface. The exchange velocities, also known as turbulent transfer coefficients, can therefore be expressed as

$$\gamma_{T,S} = C_D^{\frac{1}{2}} \Gamma_{T,S} U_a, \tag{6}$$

where $C_D^{\frac{1}{2}} \Gamma_{T,S}$ represents the thermal and haline Stanton numbers, which have been derived from laboratory studies of boundary layers on flat, smooth plates (Kader & Yaglom 1972). This parameterization is widely used in numerical models to calculate the melt rate at the front of a glacier. The expressions for the turbulent transfer coefficients have compared favorably with observations beneath sea ice (McPhee et al. 1999), including their dependence on the friction velocity. The three-equation model has been validated by observations of ablation at the base of

the Ronne Ice Shelf, which have also led to slightly modified values of the transfer coefficients (Jenkins et al. 2010).

In applying this parameterization to Greenland's glaciers, it is important to recognize that it was developed for sloping ice shelves in Antarctica and that, in particular, the validity of Equation 6 for vertical glaciers has not been tested. Thus, validation of the turbulent transfer coefficients for Greenland's glaciers with in situ observations is needed, given the strong dependence of melt rate on these coefficients. Until this validation has been done, care must be taken when using this parameterization in numerical models. One additional complication is that the turbulent transfer coefficients depend on the velocity in the ambient water near the ice-ocean interface (U_a in Equation 6). For Greenland's mostly vertical glacier fronts, this velocity is that of the buoyant plumes (see Section 3.2), which, in a model, is a strong function of the numerical resolution, with coarser resolutions resulting in slower plumes. Sensitivity studies must therefore be conducted to investigate the effects of variable resolutions on the value of U_a and consequently on the melt rate. As the model resolution is increased, progressively smaller turbulent scales are resolved, and the parameterization may need to be modified to account for this.

Glacially modified waters: a mixture of ambient water and one or two of the distinct glacial water sources, i.e., the submarine melt and the subglacial discharge

3.2. The Plume Region

The water properties at the ice front, which determine the melt rates, are strongly influenced by the presence of buoyant plumes, distributed along the glacier front, that are fed by submarine melt and/or subglacial discharge. Subglacial discharge, which occurs mostly in summer, enters the fjord waters through channels discharging at the base of the glacier's front whose number, sizes, and geometries are mostly unknown and possibly influenced by the complex networks of drainage channels and crevasses in the glaciers (for a review, see Chu 2014). From a plume modeling perspective, subglacial discharge can be represented as a buoyancy forcing at a fixed depth. Submarine melting instead occurs along the entire depth of the glacier front immersed in water. Thus, any plume model formulated to represent submarine melting must account for a buoyancy forcing distributed over a vertical area.

For Greenland's tidewater glaciers, the summer subglacial discharge volume flux, Q_{sg}, is usually much larger than the volume flux resulting from submarine melting, Q_{sm}, and, thus, in a buoyant plume forced by subglacial discharge the contribution from submarine melting is small (Sciascia et al. 2013, Xu et al. 2013). This, in turn, suggests that the near-ice dynamics in summer differ from those in winter, consistent with the evidence of seasonal differences in the exported glacially modified waters found in HG and Godthåbsfjord (Straneo et al. 2011, Mortensen et al. 2013).

Regardless of their specific forcing, these buoyant plumes rise near the glacier front, entraining ambient water, until they reach the surface or their level of neutral buoyancy (**Figure 3*b*,*c***). Once this occurs, the plume of glacially modified water detaches from the glacier front, intrudes horizontally into the ambient water, and moves away from the glacier as a buoyancy-driven current (see Section 4). The entrainment of ambient water in the rising buoyant plumes, in turn, drives a slow flow of ambient waters toward the glacier. In Greenland, highly turbid plumes reaching the surface have been detected at the margins of some tidewater glaciers (Chu et al. 2009). In other glacial fjords, studies have found evidence of mid-depth intrusions of glacially modified waters (Johnson et al. 2011, Mortensen et al. 2011, Straneo et al. 2011, Inall et al. 2014, Sutherland et al. 2014) (**Figure 2**), suggesting that the plumes associated with these intrusions were neutrally buoyant before reaching the surface. A modeling study of plumes in HG showed that, depending on the magnitude of the subglacial discharge, a plume can reach either the surface or its neutral buoyancy level at an intermediate depth (Sciascia et al. 2013) (**Figure 2*c***), as discussed in Section 3.3.

Entrainment assumption: the assumption that the entrainment velocity, w_e, is a fraction α of the vertical velocity in the plume, w

Plume buoyancy flux: $B = g'Q$, where Q is the plume volume flux; $g' = g(\rho_P - \rho_a)/\rho_0$ is the reduced gravity; ρ_P and ρ_a are the plume and ambient densities, respectively; and ρ_0 is a representative density

3.2.1. Plume theory. To understand the parameters that control the plumes' dynamics, and hence the near-ice circulation and melting, we review the basics of plume theory. The expressions derived, in turn, provide a means of assessing where the plume will reach its neutral buoyancy level (i.e., the intrusion depth) and move away from the glacier front. To do this, we build on the idealized self-similar solutions and entrainment assumption introduced by Morton et al. (1956).

Theory predicts that the evolution of plumes is controlled largely by the plumes' buoyancy forcing, which in turn regulates the amount of entrainment and mixing with the ambient fluid (Morton et al. 1956, Turner 1979). In the simplest scenario, the buoyancy forcing occurs at a fixed depth. In glacial fjords, this corresponds to a plume predominantly forced by subglacial discharge. If the ambient water density is homogeneous, then theory predicts that the plume's buoyancy flux, B, remains constant with height, z, and can therefore be calculated at the source where the reduced gravity, g', and plume volume flux, Q, are known.

If one makes the simplest entrainment assumption that the entrainment velocity, w_e, is some fraction α of the vertical velocity in the plume, w (Morton et al. 1956, Taylor 1958), then relatively simple expressions for the plumes' properties can be derived. These expressions differ depending on whether the discharge is occurring from a localized, so-called point source (i.e., a channel) or from a distributed, line source (i.e., a crack extending along the glacier front).

Given the above entrainment assumption, the equations for the conservation of mass, momentum, and buoyancy in the plume lead to expressions for the plume radius, b; vertical velocity; reduced gravity; and volume flux for a point-source plume,

$$b = \frac{6}{5}\alpha z,\ w = \frac{5}{6\alpha}\left(\frac{9}{10}\alpha B\right)^{\frac{1}{3}}\pi^{-\frac{1}{3}}z^{-\frac{1}{3}},\ g' = \frac{5B}{6\alpha}\left(\frac{9}{10}\alpha B\right)^{-\frac{1}{3}}\pi^{-\frac{2}{3}}z^{-\frac{5}{3}},$$
$$Q = \frac{6}{5}\left(\frac{9}{10}\right)^{\frac{1}{3}}\pi^{\frac{2}{3}}\alpha^{\frac{4}{3}}B^{\frac{1}{3}}z^{\frac{5}{3}}, \tag{7}$$

and a line-source plume (Linden et al. 1990),

$$b = \alpha z,\ w = (2\alpha)^{-\frac{1}{3}}\left(\frac{B}{l}\right)^{\frac{1}{3}},\ g' = (2\alpha)^{-\frac{2}{3}}\left(\frac{B}{l}\right)^{\frac{2}{3}}z^{-1},\ \frac{Q}{l} = (2\alpha)^{\frac{2}{3}}\left(\frac{B}{l}\right)^{\frac{1}{3}}z, \tag{8}$$

where l is the length of the line source. Equations 7 and 8 assume that the profiles at each height are similar and have a top-hat radial dependence (Turner 1979). The boundary conditions used are that the mass and momentum fluxes are zero at the sources, and α is the entrainment constant, the value of which is obtained from laboratory measurements and is approximately 0.13 when a top-hat radial dependence of the variables is assumed (Linden 2000). If the mass and momentum fluxes are not zero at the sources, then a small correction to Equations 7 and 8 needs to be applied to account for the finite momentum and volume fluxes (Hunt & Kaye 2001).

If the dominant buoyancy forcing of the plume is due to submarine melting (as is likely the case in winter and away from regions of subglacial discharge in summer), then the plume is forced over an area of width l and height H. If we assume that the submarine melting provides a buoyancy flux per unit area $\Phi = B/lH$ and zero fluxes of volume and momentum, then a similar approach to that of Morton et al. (1956) for point sources of buoyancy can be used to derive the self-similar solutions in a uniform-density ambient water (Cooper & Hunt 2010):

$$b = \frac{3}{4}\alpha z,\ w = \left(\frac{4}{5}\right)^{\frac{1}{3}}\alpha^{-\frac{1}{3}}\Phi^{\frac{1}{3}}z^{\frac{1}{3}},\ g' = \frac{4}{3}\left(\frac{5}{4}\right)^{\frac{1}{3}}\alpha^{-\frac{2}{3}}\Phi^{\frac{2}{3}}z^{-\frac{1}{3}},$$
$$\frac{Q}{l} = \frac{3}{4}\left(\frac{4}{5}\right)^{\frac{1}{3}}\alpha^{\frac{2}{3}}\Phi^{\frac{1}{3}}z^{\frac{4}{3}}. \tag{9}$$

The assumption of zero flux of volume can be justified given that the entrained volume flux, Q_e, is much larger than the volume flux resulting from submarine melting, i.e., $Q_{sm} \ll Q_e$.

3.2.2. Intrusion depth. The self-similar solutions obtained in the previous section allow us to estimate the depth at which the buoyant plumes will detach from the glacier front and intrude horizontally into the ambient stratified water. Although the following argument can be carried over for any general stratification of the ambient water, for simplicity, we assume the stratification to be two layers, with the bottom layer having density ρ_B and depth H_B and the top layer having density ρ_T and depth H_T. The flow rate of entrained ambient water can be defined as

$$Q_e(z') = \int_{A_p} w_e \mathrm{d}A, \tag{10}$$

where A_p is the area through which entrainment occurs and differs for line, point, and vertical plane plumes. The density of the plume at a depth z' above the source is (Sciascia et al. 2013)

$$\rho_P(z') = \frac{\rho_{P0} Q_{sg} + \rho_B Q_e}{Q_{sg} + Q_e}, \tag{11}$$

where ρ_{P0} is the plume density at the source. Alternatively, using the expressions in Equations 7, 8, and 9 for the reduced gravity, the density of the plume at a depth z is

$$\rho_P(z) = \frac{\rho_0}{g} g'(z) + \rho_B. \tag{12}$$

For a two-layer stratification, the buoyant plume penetrates the interface between the two layers if the density of the plume at the interface, $\rho_P(z = H_B) = \rho_I$, is lower than the density of the upper layer, i.e., $\rho_I < \rho_T$ (**Figure 3*c***). In this scenario, the freshwater flux in the buoyant plume reaches the free surface and is found in the fjord surface layer. However, if $\rho_I > \rho_T$, then the buoyant plume is not able to reach the free surface, and it intrudes in the fjord waters at depth, along the interface. Therefore, to predict the amount of freshwater flux, Q_f, and the location of the freshwater in the fjord water column, correctly representing the source geometry and buoyancy flux of the plumes is essential.

3.3. Models of Plumes and Glacier Melting

The use of simplified one-dimensional models based on the theory of buoyant plumes has led to some progress in understanding the dynamics near a glacier front (Hellmer & Olbers 1989; Jenkins 1991, 2011). These models use the same equations for the conservation of mass, momentum, heat, and salt as were used to obtain the self-similar solutions described in Section 3.2.1, but with additional terms to account for melting and freezing at the ice-ocean interface and the resulting input or extraction of freshwater (Section 3.1). These models are steady in time, uniform in the across-flow direction, and integrated along the width of the buoyant plume, resulting in a one-dimensional model in which the plume thickness, speed, temperature, and salinity vary with depth. They are closed using a constant drag coefficient and a linear equation of state. These one-dimensional models have proven successful in estimating the dependence of the submarine melting on several variables, for example, the ambient water temperature and subglacial discharge (Jenkins 2011).

The melt rate parameterization of the ice front based on the three-equation model with velocity-dependent turbulent transfer coefficients has also been used in the MIT General Circulation Model to simulate submarine ice shelf melting in Antarctica (Losch 2008, Heimbach & Losch 2012, Schodlok et al. 2012, Dansereau et al. 2014) and to evaluate submarine melting in Greenland tidewater glaciers (Xu et al. 2012, 2013; Sciascia et al. 2013, 2014). Depending on

the resolution, the plume dynamics and the entrainment processes are either completely or partially parameterized by a diffusive flux (even with grid size ∼5 m). Therefore, caution must be used in determining whether the entrainment process is parameterized appropriately through the diffusion formulation. Sciascia et al. (2013) showed that for a given value of the Laplacian eddy diffusivity, the implied entrainment flux is appropriate only within a range of parameters.

4. FJORD-SCALE CIRCULATIONS

At the fjord scale, the circulation is influenced by tides, buoyancy forcing from the glacier and icebergs, surface fluxes, local winds, and exchange with the continental shelf through the mouth of the fjord. The reviews cited above include extensive discussions of how the fjord circulation is forced by tides, along-fjord winds (which can be particularly intense in glacial fjords; Oltmanns et al. 2014), and surface fluxes; here, we focus on a subset of circulations that are likely dominant in large glacial fjords.

4.1. Buoyancy-Driven Circulation

Freshwater discharged from tidewater glaciers forces a buoyancy-driven circulation that is analogous to the estuarine circulation found in many estuaries and fjords, but with some important differences. The classic estuarine circulation is driven by the release of freshwater at the surface, Q_{sf}, usually at the head of the fjord, and turbulent mixing caused by winds, tides, and other processes (Farmer & Freeland 1983, Stigebrandt 2012). The turbulence mixes the freshwater downward, entraining ambient fjord water and generating an inflow of denser (typically saltier) waters beneath the outflowing fresher layer (**Figure 4**, purple). Theories relating the magnitude of the estuarine circulation to the fjord's parameters, mixing, and Q_{sf} have been proposed for several special cases: hydraulic control at the sill (Stommel & Farmer 1953), deep lower-layer and wind-driven mixing (Stigebrandt 1981), and partially mixed estuaries (MacCready & Geyer 2010).

In a glacial fjord, buoyancy-driven flows are similarly associated with a freshwater discharge, Q_f, of total magnitude $Q_f = Q_{sf} + Q_{sg} + Q_{sm}$. Unlike typical estuarine systems, however, two of these terms, Q_{sg} and Q_{sm} (the subglacial discharge and the submarine melt, respectively), involve the discharge of freshwater at depth and result in turbulent plumes that entrain ambient water as they rise (Section 3.2).

Motyka et al. (2003) proposed a steady-state model for the estuarine circulation near LeConte Glacier, Alaska. This model assumes that $Q_{sf} \ll Q_{sg} + Q_{sm}$ and that the fjord can be described as a single ambient fjord water mass plus the overlying freshwater originating from the glacier, as is often done for fjords with shallow sills. Conservation of mass and salt for this model can be written via the Knudsen equations:

$$Q_1 = Q_2 + Q_f \approx Q_2 + Q_{sg} + Q_{sm}, \tag{13}$$

$$Q_1 S_1 = Q_2 S_2, \tag{14}$$

where Q is the volume flux, S is the salinity, and the subscripts 1 and 2 indicate the upper, fresh layer and the lower, salty layer, respectively. Assuming that submarine melting and the addition of subglacial discharge are the only heat sink/source terms within the fjord and that the system is in steady state, Motyka et al. (2003) expressed conservation of heat as

$$\rho_1 C_1 Q_1 \theta_1 = \rho_1 C_2 Q_2 \theta_2 + \rho_{fw} C_{fw} Q_{sg} \theta_{sg} + Q_{sm} L, \tag{15}$$

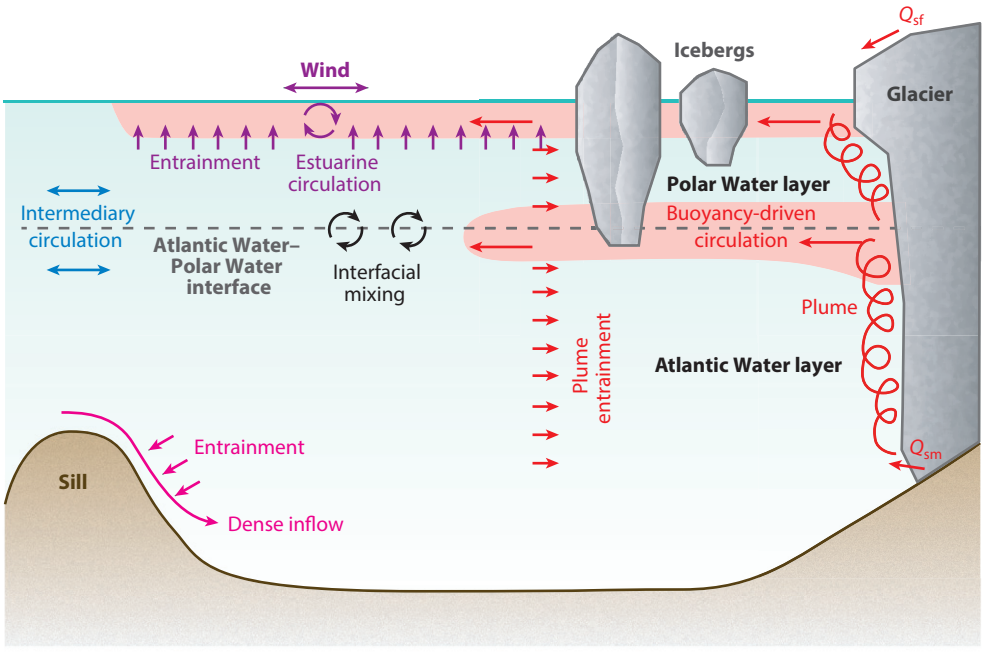

Figure 4

Schematic representation of the different circulations in a Greenland glacial fjord. Red indicates the buoyancy-driven circulation resulting from the submarine melting, subglacial discharge, and surface runoff; purple the estuarine circulation resulting from surface runoff only; blue the intermediary baroclinic circulation; and pink the circulation generated by the dense inflow over the sill.

where C is the specific heat capacity of water, θ is the potential temperature, L is the latent heat of fusion, ρ is the density, and the subscripts sg, fw, and sm indicate subglacial discharge, freshwater, and submarine melt, respectively.

The applicability of simplified models such as Motyka et al.'s (2003) to Greenland's fjords, however, is problematic. These fjords are characterized by a strongly stratified (owing to AW and PW) ambient water column that can give rise to intrusions of glacially modified water at mid-depths, typically between the AW and PW layer, both in winter and in summer (Mortensen et al. 2011, Straneo et al. 2011, Sutherland et al. 2014) (**Figure 2*a*,*b***). Thus, we expect the buoyancy-driven flow in Greenland's fjords to be best described as a three- or four-layer system rather than a two-layer system (**Figure 4**, red). In addition, as discussed in Section 5, the extent to which steady-state assumptions are valid for Greenland's fjords is still in question.

Numerical simulations of the buoyancy-driven circulation in fjords have confirmed the importance of subglacial discharge. Depending on its magnitude, this discharge can give rise to a single overturning cell (when it reaches the surface) or multiple cells (when some of it intrudes at mid-depth; **Figure 3*c***) (Sciascia et al. 2013; Xu et al. 2012, 2013). In a realistic setting, we expect multiple drainage channels and a strongly three-dimensional circulation near the glacier edge, where multiple plumes interact. This in turn modifies the plumes' dynamics and entrainment (Cenedese & Linden 2014) and consequently the submarine melt rate (Xu et al. 2013, Kimura et al. 2014). As one moves progressively away from the glacier, however, lateral mixing resulting from

a variety of processes is likely to reduce lateral gradients, resulting in a more two-dimensional circulation with negligible across-fjord variations. A recent numerical study suggests that the buoyancy-driven flow can account for the flushing of JI on annual or shorter timescales (Gladish et al. 2014).

4.2. Intermediary Circulation

Intermediary flows are shelf-driven flows that occur above the sill depth. They are driven by density variations outside the fjord, which can originate from along-shore winds (upwelling or downwelling) or density anomalies advected past the mouth of the fjord. The fjord/shelf density contrasts result in horizontal pressure gradients that drive baroclinic flows (Svendsen 1980, Klinck et al. 1981, Stigebrandt 1990) (**Figure 4**, blue). In narrow fjords, this gives rise to vertically sheared flows across the entire width. In wide fjords, rotational effects result in geostrophic flows within the fjords. Intermediary circulations are highly effective at flushing the waters above the sill depth and can be an order of magnitude larger than estuarine flows (Stigebrandt 1990).

Several studies have recently confirmed the importance of intermediary circulations in Greenland's deep-silled fjords. These circulations were first invoked to explain the renewal of the upper 400 m of HG within two months (Straneo et al. 2010) and then were later used to explain the strongly sheared velocities, reversing every few days, measured in HG and KG (Sutherland & Straneo 2012, Sutherland et al. 2014). More recently, moored data from HG and KG showed that intermediary circulations dominate the circulation and variability during the non-summer months (September to May), are driven by density fluctuations outside the fjord that are often (but not always) associated with downwelling wind events, and can result in rapid changes in fjord properties owing to advection from the shelf region (Jackson et al. 2014) (**Figure 5**). Mortensen et al. (2011) also described intermediary flows for Godthåbsfjord.

Given the two-layer character of the shelf waters (i.e., the presence of dense AW and light PW), that intermediary circulations are important in Greenland's large fjords is perhaps not surprising. Fjords with sills deeper than the AW-PW interface (e.g., **Figure 1**) allow for a relatively unobstructed exchange of AW and PW between the shelf and the fjord. Thus, any fluctuation of the AW-PW interface on the shelf will drive intermediary flows. An analysis of the variability of the shelf properties outside of HG using moored data showed that 60% of the submonthly variability is associated with along-shore, downwelling winds (known as barrier winds in this region), whereas the rest is attributed to variability in the East Greenland Coastal Current, which is advected into the region (Harden et al. 2014).

Stigebrandt & Aure (1990) developed an empirical model of intermediary circulation for fjords along the Norwegian coast. This model expresses the volume flux in each layer (the vertically integrated volume flux resulting from the intermediary circulation is zero) at the fjord's mouth as

$$Q_{\mathrm{int}} = \beta (g W_{\mathrm{m}} H_{\mathrm{s}} A_{\mathrm{f}} \Delta M / \rho_0)^{\frac{1}{2}}, \tag{16}$$

where W_{m} is the width of the mouth, H_{s} is the sill depth, A_{f} is the horizontal area of the fjord at the sea surface, and β is an empirically derived constant ($\beta = 17 \times 10^{-4}$ was found to achieve the best fit for Norwegian fjords). The forcing for the intermediary circulation, ΔM, is given by the standard deviation of the weight M (in kilograms per square meter) of a water column extending

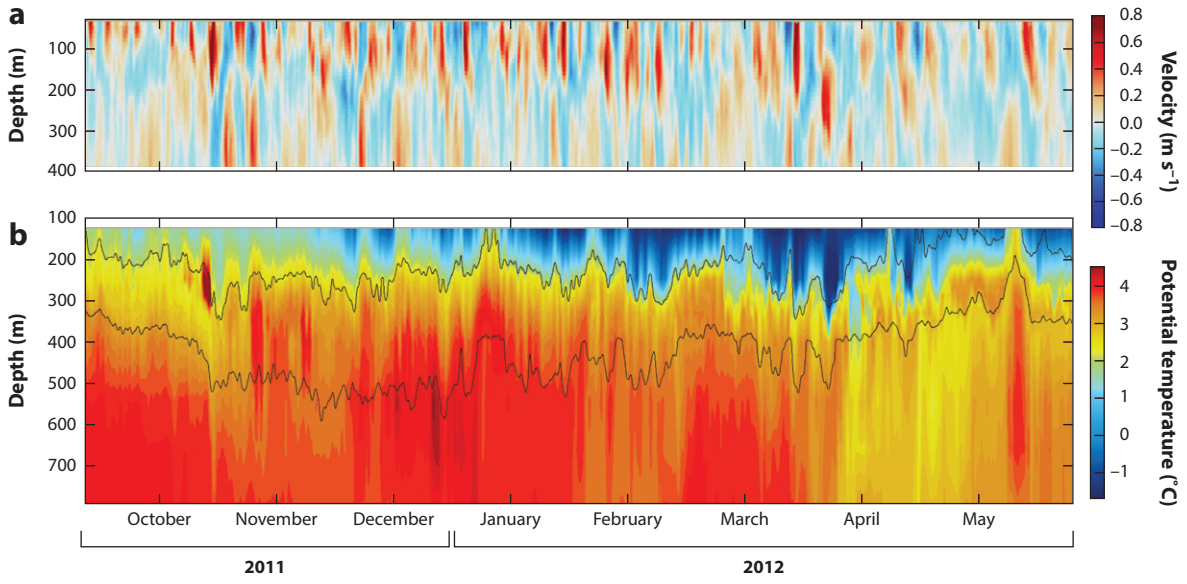

Figure 5

High-frequency variability in Sermilik Fjord (Helheim Glacier) from moored observations: (*a*) along-fjord velocity (positive is toward the glacier) and (*b*) potential temperature from a mooring located in the middle of the fjord (white star in **Figure 2*c***). Two isopycnals ($\sigma_\theta = 27$ and 27.5 kg/m^3) are overlaid. Figure modified from Jackson et al. (2014).

from the mean sea surface, η, to the sill depth (Aure et al. 1996, Stigebrandt 2012):

$$\Delta M = \int_{-H_s}^{\eta} \sigma_\rho(z)\mathrm{d}z, \tag{17}$$

where σ_ρ is the standard deviation of $\rho(z)$. Different models exist for fjords in which rotation is important or the flow is hydraulically controlled (Stigebrandt 1990). Although Equation 17 does not contain information about the forcing period, Aure et al. (1996) suggested that the relevant frequencies are the subseasonal ones and that higher frequencies, on the order of days, are more effective drivers. Arneborg (2004) proposed an alternative expression for the exchange rate, E, based on observations of isopycnal displacement inside the fjord:

$$E = Q_{\mathrm{int}}/V = \Delta b/H_s t, \tag{18}$$

where V is the fjord volume above the sill depth, Δb is the amplitude of the isopycnal displacements inside the fjord, and t is the characteristic forcing period. Using parameters from HG (inferred in part from **Figure 5**), such that $\Delta b \sim 50$ m, $H_s \sim 600$ m, and $t = 5$ days, we get $E = 1/(60$ days). In other words, this model predicts that the baroclinic fluctuations observed in HG will tend to flush the upper 600 m of the fjord waters within two months, consistent with the findings of Straneo et al. (2010) and Jackson et al. (2014).

Another important role of intermediary flows is their ability to advect shelf anomalies into the fjord on submonthly timescales (Jackson et al. 2014). This may explain the interannual changes observed in several fjords—e.g., Godthåbsfjord (Mortensen et al. 2013) and KG (Christoffersen et al. 2011). These changes would be much harder to justify based on an estuarine-type circulation alone (Sutherland et al. 2014).

Given that intermediary flows likely control the renewal of waters in the fjord and contribute to mixing, they likely also have an impact on both submarine melting and the export of freshwater,

as proposed in the idealized numerical study by Sciascia et al. (2014). However, more in-depth studies of how these flows interact with fully turbulent and three-dimensional plumes in the near-ice region are needed to investigate the impact of these flows on submarine melting and on the freshwater export.

4.3. Deep-Water Renewal

The deep water, below sill depth, is periodically renewed by the inflow of denser water from the shelf over the sill, which entrains relatively fresher water from above (**Figure 4**, pink). For nonglacial fjords, the residence time of the deep water below sill level is thought to depend on the mixing rate, the intermediary flows, and the volume of water below sill level (Stigebrandt 2012).

For Greenland's glacial fjords, where subglacial discharge and submarine melting introduce freshwater at depth, one might expect the residence time to be reduced relative to that of a nonglacial fjord owing to the entrainment of deep water into the buoyant plumes. A tracer-based estimate of deep-water residence time for the waters below the 300-m sill of PG indicates a ventilation time of 30 years (Johnson et al. 2011). By contrast, Jackson et al. (2014) showed that even at 900 m, the waters of HG undergo rapid variations in properties, suggesting a renewal on the order of months, which, for HG, is likely tied to the vigorous intermediary flow. Based on annual summer surveys in JI, Gladish et al. (2014) concluded that waters below sill depth are renewed on timescales of a year or shorter and suggested, using a numerical model, that this renewal can be achieved by a buoyancy-driven circulation alone. These seemingly diverging conclusions are indicative of our limited understanding of processes governing the renewal of water in the fjords as well as the transport of heat toward the glacier and export of glacially modified waters.

5. SUBMARINE MELTING

Estimates of submarine melt rates and their controls are crucial to understanding glacier behavior, yet direct observations are impractical because of the challenges of collecting data near calving fronts and under long floating ice tongues. For long floating ice tongues, submarine melt rates have been estimated using ice flux divergence methods, yielding ∼10 m/y for PG (Münchow et al. 2014 and references therein), ∼8 m/y for 79NG (Mayer et al. 2000), and ∼238 m/y for JI before it lost its ice tongue (Motyka et al. 2011). For rapidly calving glaciers, distinguishing submarine melting from calving gives rise to larger uncertainties. One recent ice flux–based study of 13 glaciers suggested that submarine melt rates can vary from ∼10 to 1,000 m/y (Enderlin & Howat 2013). A different approach is to estimate melt rates and identify their controls from fjord observations or models of fjord circulation.

5.1. Heat Flux to the Glaciers

Submarine melting is associated with a net flux of heat from the ambient fjord water to the glacier. Thus, in principle, estimating this heat flux would also provide an indirect estimate of the submarine melt rate. Consider a volume of a fjord, V_x, of width W enclosed by the glacier at one end (grounding line is at $x = 0$) and a section perpendicular to the fjord's axis located at a distance $x = x_V$ from the grounding line. The conservation of heat for V_x is

$$\frac{\partial}{\partial t}\iiint_{V_x}(\rho_{sw}C_{sw}\theta_{sw})\mathrm{d}x\mathrm{d}y\mathrm{d}z + \int_0^W\int_{-H}^0 \rho_{sw}C_{sw}U\,\theta_{sw}(x,y,z,t)\mathrm{d}y\mathrm{d}z$$
$$= \rho_i Q_{im}[L_i + C_i(\theta_i - \theta_f)] + \rho_{fw}C_{fw}Q_{sm}\theta_{sm} + \rho_{fw}C_{fw}Q_{sg}\theta_{sg} + \Lambda, \quad (19)$$

where the first term on the left-hand side is the rate of heat content change in V_x, the second term on the left-hand side is the heat flux across the section at $x = x_V$, and the three right-hand terms are the heat sink/source terms: the heat used to melt the glacier (which includes warming the ice to its freezing point; see sidebar, Ice Melting in Ocean Water sidebar), the heat sink/source term resulting from the subglacial discharge, and any additional heat flux, Λ (e.g., air-sea fluxes or the melting of icebergs). U is the velocity perpendicular to the section at $x = x_V$; Q_{sm} and Q_{im} are the volume fluxes of liquid water and ice melt, respectively ($\rho_w Q_{sm} = \rho_i Q_{im}$); and the subscripts sw, i, fw, sg, and f indicate seawater, ice, freshwater, subglacial discharge, and freezing, respectively.

The heat balance in the Motyka et al. (2003) model, Equation 15, is a special case of Equation 19 with an additional constraint taken from conservation of salt. First, they assume that the change in the heat content in V_x is negligible (i.e., steady state). Second, the heat sink/source terms are limited to submarine melting ($\Lambda = 0$, $\theta_{sg} = 0$). Then, to estimate the velocity, they assume that the system can be represented as a two-layer estuarine system where volume and salt conservation can be written via the Knudsen equations (Section 4.1).

Other simplified forms of Equation 19, typically supplemented by synoptic velocity data collected across a fjord section and often including forms of volume and/or salt conservation, have recently been used to infer submarine melt rates from summer surveys at the margins of several Greenland glaciers (Rignot et al. 2010, Sutherland & Straneo 2012, Xu et al. 2013, Inall et al. 2014), yielding values that range from 200 to 3,650 m/y (though these estimates apply only to summer). In all cases, changes in heat content in the fjord volume, V_x, are neglected, and it is assumed that the inferred heat transport is going into melting ice. This assumption is dictated largely by the lack of appropriate data to estimate changes in heat content in V_x along with other heat source/sink terms. In principle, if there exists a timescale over which V_x's properties can be assumed to be steady and one averaged the heat flux toward the glacier over this period of time, and assuming other external sink/source terms are negligible, then one could derive the net heat transport to the glacier. In practice, it is unclear whether such a timescale exists, given the strong seasonality imparted by the subglacial discharge to the buoyancy-driven flow and the high-frequency variability that may result from intermediary flows. It definitely seems unlikely that fjord surveys lasting a few days can provide adequate information on a time-averaged circulation.

One further complication in using the heat flux method to estimate submarine melt rate is quantifying the heat flux itself (i.e., the second term on the left-hand side of Equation 19). Velocity measurements in Greenland's glacial fjords are difficult to obtain, and most studies rely on some simplification to extrapolate the velocity field across a fjord cross section, such as assuming that the flow is geostrophic (Johnson et al. 2011 for PG, Inall et al. 2014 for KG) or that it consists of a two-layer estuarine cell (Rignot et al. 2010, Xu et al. 2013). In most cases, however, there is little evidence to support the assumptions made. One attempt to estimate the residual, heat-transporting circulation relied on removing the higher-frequency (intermediary) mode (Sutherland & Straneo 2012). Using this residual velocity to estimate the heat flux toward the glacier involves making two assumptions, however: first, that the slowly varying, heat-transporting mode does not project onto the mode that was filtered out, and second, that higher-frequency modes themselves do not contribute to the heat transport to the glacier. At present it is unclear to what extent these assumptions can be justified.

The few existing continuous (moored) velocity observations from the fjords do not support several of the assumptions made in simplifying Equation 19. These observations showed that the heat content within the fjords varies considerably over timescales of several days and longer, consistent with rapid changes in circulation (Jackson et al. 2014) (**Figure 5**). The implication is that much of the heat flux through a section over periods of days will go into warming or cooling V_x rather than melting ice. Even when long-term averages can be obtained, these do not necessarily

yield a net heat flux to the glacier. For example, an analysis of a nine-month-long moored record during the non-summer months from HG still failed to produce a significant estimate of a heat flux (Jackson et al. 2014). The assumption of two-layer estuarine circulation is also problematic, given that mid-depth intrusions of glacially modified waters are observed in several fjords. In general, exactly what circulation is transporting heat to the glacier remains unclear. Finally, other sink terms need to be evaluated more carefully. Iceberg melting is likely a major heat sink in fjords with rapidly calving glaciers. A recent study estimated the submarine melt rate of icebergs in HG to be ∼140 m/y (Enderlin & Hamilton 2014), which, given the large number of large icebergs near some of these glaciers, implies that the iceberg melt term is likely a major term in the fjord's heat budget. Air-sea fluxes, including sea ice formation, may also play a role in the heat balance of the fjord systems, especially during winter.

5.2. Submarine Melt Rates from Numerical Models

When used in conjunction with a thermodynamical melt rate parameterization (e.g., Losch 2008), ocean models provide an alternative method for estimating melt rates. The idea behind this approach is to use a numerical, or theoretical, model to describe the near-ice circulation and the ice-ocean exchange. The required inputs are the glacier characteristics, the subglacial discharge (the number and size of drainage channels and the fluxes out of them), the ocean forcing at the far boundary (the mouth of the fjord, the shelf, or where the model domain ends), any additional forcing that is relevant to the problem studied (e.g., surface fluxes), and parameterizations of unresolved turbulent processes, including the ice-ocean boundary parameterization (see Section 3.1). One major advantage of these models is that they can be used to estimate the spatial (i.e., along the glacier face) and temporal variability of the submarine melt rate. These models have been used to estimate the melt rates for JI (Jenkins 2011), HG (Sciascia et al. 2013), and Store Glacier (Xu et al. 2013), yielding ranges of ∼70–1,100 m/y. Collectively, these studies suggest that the submarine melt rate increases with increasing subglacial discharge (with a power of 1/3), linearly increases with increasing temperature, and increases with vertical distance above the grounding line in winter and slightly decreases with it in summer.

In summary, numerical models clearly provide a key tool for determining which processes influence submarine melting and its variability. At the same time, though, it is important to acknowledge that the magnitude and the spatial and temporal variability of the submarine melt rates derived from the models are highly sensitive to the parameterizations employed—including the ice-ocean boundary layer parameterization, whose parameters and coefficients have yet to be validated by measurements (see Section 3.1)—and to largely unknown external forcings such as the subglacial discharge. As such, caution must be exercised to avoid putting too much weight on the models' quantitative results.

6. FRESHWATER DISCHARGE

The GrIS total freshwater discharge into the ocean is given by the sum of ice discharge (icebergs and submarine melting) and runoff of ice melting above sea level. During the period 1961–1990, the GrIS was mostly stable, with an estimated ice discharge of 497 ± 50 km^3/y and runoff of 416 ± 57 km^3/y (Bamber et al. 2012), equivalent to a total freshwater discharge of 0.029 ± 0.002 sverdrups (Sv). Both these components have increased over the past two decades, and a recent study estimated that the additional (ice and runoff combined) freshwater discharge in 2012 was 378 ± 50 km^3/y (Enderlin et al. 2014), resulting in a total freshwater discharge of 1,291 ± 50 km^3/y, i.e., a net transport into the ocean of 0.041 ± 0.002 Sv. These numbers are obtained by separately estimating the two different components. The ice discharge is calculated by deriving the

ice flux through a flux gate near the glaciers' termini using thicknesses and speeds inferred from airborne and remote sensing products. The runoff is computed using a high-resolution (~11 km) regional climate model (including an atmosphere and a snow pack) forced at its boundaries by reanalysis products (e.g., van den Broeke et al. 2009).

Most of Greenland's freshwater is discharged at the margins of the subpolar North Atlantic and the connected Baffin Bay (Bamber et al. 2012). The freshwater enters the ocean as a result of the combined calving, submarine melt, and subglacial discharge that occur at the head of the glacial fjords. Thus, the fjords are the conduits through which this freshwater eventually reaches the boundary currents on the continental shelves of Greenland. As discussed above, this freshwater flux from the GrIS is not distributed evenly around Greenland but instead is localized into a discrete number of points, corresponding to the major glacial fjords. Furthermore, the bulk of the liquid discharge (i.e., the subglacial discharge) occurs at depth, at the grounding line of the glaciers rather than at the surface.

From the perspective of the large-scale ocean circulation as well as the ocean and climate models, the freshwater discharge from Greenland is that exported from the fjords, where fjord processes can act to transform (for example, by mixing) or delay (for example, by storing) the glacier freshwater input. If the fjords' dynamics are not resolved, appropriate boundary conditions for Greenland's freshwater must account for modification of the temporal and spatial freshwater distribution caused by the fjord's processes through appropriate parameterizations. Based on the results summarized in this review, one expects the following. First, a significant portion of the subglacial discharge released at depth is likely to remain subsurface and to emerge as glacially modified waters that spread beneath the PW. Thus, counter to the common assumption when prescribing freshwater boundary conditions from Greenland, not all of this discharge can be assumed to be a surface flux. Second, the highly seasonal liquid discharge is likely to impart a strong seasonal variability to the freshwater export, and fjord processes may delay this export by weeks or longer timescales depending on the magnitude of the fjord's circulation. For the solid portion, some of the icebergs will melt while residing in the fjords. If these are deep (e.g., below the AW-PW interface), then one expects that some of this meltwater will be trapped subsurface, as with the subglacial discharge. The melt rate within the fjords, in turn, will depend on the residence times of icebergs, which likely vary from fjord to fjord. The ensemble of the fjord dynamics and their impact on the freshwater discharge from Greenland must thus be determined before appropriate boundary conditions can be formulated for large-scale ocean and climate models.

SUMMARY POINTS

1. Greenland's glacial fjords constitute a key link between the ocean and the ice sheet. Understanding their dynamics—particularly submarine melting at the glaciers' edges and the export of freshwater—will be important for understanding and predicting Greenland's changes and their impact on the climate/ocean.
2. Theories developed for other fjord systems are not immediately applicable to Greenland's glacial fjords because of the different parameter ranges of the latter, which include deep sills, Atlantic and Polar Waters, and large volumes of subglacial discharge.
3. Buoyancy-driven flows in Greenland's fjords have a strong seasonality because of the discharge of surface melt at the base of the glacier in summer. These flows are also strongly influenced by the fjords' stratification, which allows mid-depth intrusions of glacially modified waters.

4. Shelf-driven intermediary flows are important for Greenland's deep-silled fjords and drive a rapid and continuous renewal of the fjords' waters. The transport associated with these flows is much larger than that associated with buoyancy-driven flows, but how they contribute to the heat transport to the glacier is unclear.
5. The fjord circulation is likely determined by the interaction of the intermediary flows with the buoyancy-driven flows. At present there is no simple theory that combines these two circulations and predicts which mode may dominate in a particular fjord.
6. Our understanding of processes at the ice-ocean boundary is strongly influenced by existing parameterizations that are largely untested in the dynamical regimes pertinent to Greenland.
7. Estimates of submarine melt rates are still highly uncertain. Estimates based on fjord data suffer from the challenges of obtaining appropriate velocity and property measurements, including taking them over appropriate time periods. Submarine melt rates derived from numerical models using ice-ocean boundary parameterizations depend strongly both on the model's ability to account for the plumes' dynamics and on the choice of the turbulent transfer coefficients used in the parameterizations. Furthermore, both methods require knowing the characteristics of the glacial discharge, which are challenging to observe for Greenland's glaciers.
8. Freshwater discharge from Greenland enters the large-scale ocean not only at the surface but also at depth as a result of the fjord's vertical stratification and the discharge of surface melt at the bases of the deeply grounded glaciers. The distribution of this freshwater discharge around Greenland's margin varies greatly because of the channeling of freshwater through the fjords.

FUTURE ISSUES

1. Key measurements and modeling of the turbulent processes and their controls are needed to establish the characteristics of the ice-ocean boundary layer. Testing of existing and new parameterizations by combining direct submarine melt rate observations with theoretical predictions is key to assessing their validity. A related problem is the appropriate choice of large-scale variables in these parameterizations.
2. Knowledge of the spatial and temporal variability of subglacial discharge and its influence on the near-ice circulation is key to estimating submarine melt rates and freshwater export.
3. Repeat and long-term observations from different glacial fjords, spanning across different regimes, are needed to inform our understanding and guide model development. Indeed, many of the recent advances in our knowledge have derived from observations.
4. Understanding the interactions of buoyancy-driven and shelf-driven flows within glacial fjords is necessary to understand the physical controls on submarine melt rates and freshwater export.

5. An improved understanding of the glacial fjord dynamics in Greenland will lead to adequate parameterizations of fjord processes, which can then provide adequate forcing for ice sheet or ocean/climate models.

DISCLOSURE STATEMENT

The authors are not aware of any affiliations, memberships, funding, or financial holdings that might be perceived as affecting the objectivity of this review.

ACKNOWLEDGMENTS

The authors would like to acknowledge insightful discussions with R. Jackson, D. Sutherland, P. Heimbach, and L. Arneborg. Funding for this work was provided by the National Science Foundation (grant OCE-1130008), the National Aeronautics and Space Administration (grant NNX13AK88G), and the Woods Hole Oceanographic Institution's Ocean and Climate Change Institute.

LITERATURE CITED

Amundson JM, Fahnestock M, Truffer M, Brown J, Lüthi MP, Motyka RJ. 2010. Ice mélange dynamics and implications for terminus stability, Jakobshavn Isbræ, Greenland. *J. Geophys. Res.* 115:F01005

Andresen CS, Straneo F, Ribergaard MH, Bjørk AA, Andersen TJ, et al. 2012. Rapid response of Helheim Glacier in Greenland to climate variability over the past century. *Nat. Geosci.* 5:37–41

Arneborg L. 2004. Turnover times for the water above sill level in Gullmar Fjord. *Cont. Shelf Res.* 24:443–60

Aure J, Molvær J, Stigebrandt A. 1996. Observations of inshore water exchange forced by a fluctuating offshore density field. *Mar. Pollut. Bull.* 33:112–19

Bamber J, van den Broeke M, Ettema J, Lenaerts J, Rignot E. 2012. Recent large increases in freshwater fluxes from Greenland into the North Atlantic. *Geophys. Res. Lett.* 39:L19501

Born EW, Böcher J, eds. 2001. *The Ecology of Greenland*. Nuuk, Greenl.: Ilinniusiorfik

Cenedese C, Linden PF. 2014. Entrainment in two coalescing axisymmetric turbulent plumes. *J. Fluid Mech.* 752:R2. doi: 10.1017/jfm.2014.389

Christoffersen P, Mugford RI, Heywood KJ, Joughin I, Dowdeswell JA, et al. 2011. Warming of waters in an East Greenland fjord prior to glacier retreat: mechanisms and connection to large-scale atmospheric conditions. *Cryosphere* 5:701–14

Chu VW. 2014. Greenland Ice Sheet hydrology: a review. *Prog. Phys. Geogr.* 38:19–54

Chu VW, Smith LC, Rennermalm AK, Forster RR, Box JE, Reehy N. 2009. Sediment plume response to surface melting and supraglacial lake drainages on the Greenland ice sheet. *J. Glaciol.* 55:1072–82

Church JA, White NJ, Konikow LF, Domingues CM, Cogley JG, et al. 2011. Revisiting the Earth's sea-level and energy budgets from 1961 to 2008. *Geophys. Res. Lett.* 38:L18601

Cooper P, Hunt GR. 2010. The ventilated filling box containing a vertically distributed source of buoyancy. *J. Fluid Mech.* 646:39–58

Cottier FR, Nilsen F, Skogseth R, Tverberg V, Svendsen H, Skardhamar J. 2010. Arctic fjords: a review of the oceanographic environment and dominant physical processes. In *Fjord Systems and Archives*, ed. JA Howe, WEN Austin, M Forwick, M Paetzel, pp. 35–50. London: Geol. Soc. Lond.

Dansereau V, Heimbach P, Losch M. 2014. Simulation of subice shelf melt rates in a general circulation model: velocity-dependent transfer and the role of friction. *J. Geophys. Res.* 119:1765–90

Das SB, Joughin I, Behn MD, Howat IM, King MA, et al. 2008. Fracture propagation to the base of the Greenland Ice Sheet during supraglacial lake drainage. *Science* 320:984–86

Enderlin EM, Hamilton GS. 2014. Estimates of iceberg submarine melting from high-resolution digital elevation models: application to Sermilik Fjord, East Greenland. *J. Glaciol.* In press

Enderlin EM, Howat IM. 2013. Submarine melt rates for floating termini of Greenland outlet glaciers (2000–2010). *J. Glaciol.* 59:67–75

Enderlin EM, Howat IM, Jeong S, Noh M-J, van Angelen JH, van den Broeke MR. 2014. An improved mass budget for the Greenland ice sheet. *Geophys. Res. Lett.* 41:866–72

Farmer D, Freeland H. 1983. The physical oceanography of fjords. *Prog. Oceanogr.* 12:147–220

Gade HG. 1979. Melting of ice in sea water: a primitive model with application to the Antarctic ice shelf and icebergs. *J. Phys. Oceanogr.* 9:189–98

Gladish CV, Holland DM, Rosing-Asvid A, Behrens JW, Boje J. 2014. Oceanic boundary conditions for Jakobshavn Glacier: part I. Variability and renewal of Ilulissat Icefjord Waters, 2001–2014. *J. Phys. Oceanogr.* In press. doi: 10.1175/JPO-D-14-0044.1

Harden B, Straneo F, Sutherland D. 2014. Moored observations of synoptic and seasonal variability of the East Greenland Coastal Current. *J. Geophys. Res.* In press

Heimbach P, Losch M. 2012. Adjoint sensitivities of sub-ice shelf melt rates to ocean circulation under Pine Island Ice Shelf, West Antarctica. *Ann. Glaciol.* 53:59–69

Hellmer HH, Olbers DJ. 1989. A two-dimensional model for the thermohaline circulation under an ice shelf. *Antarct. Sci.* 1:325–36

Holland DM, Jenkins A. 1999. Modeling thermodynamic ice–ocean interactions at the base of an ice shelf. *J. Phys. Oceanogr.* 29:1787–800

Holland DM, Thomas RH, de Young B, Ribergaard MH, Lyberth B. 2008. Acceleration of Jakobshavn Isbræ triggered by warm subsurface ocean waters. *Nat. Geosci.* 1:659–64

Hunt GR, Kaye NB. 2001. Virtual origin correction for lazy turbulent plumes. *J. Fluid Mech.* 435:377–96

Inall ME, Gillibrand PA. 2010. The physics of mid-latitude fjords: a review. In *Fjord Systems and Archives*, ed. JA Howe, WEN Austin, M Forwick, M Paetzel, pp. 17–33. London: Geol. Soc. Lond.

Inall ME, Murray T, Cottier FR, Scharrer K, Boyd TJ, et al. 2014. Oceanic heat delivery via Kangerdlugssuaq Fjord to the south-east Greenland ice sheet. *J. Geophys. Res.* 119:631–45

Jackson RH, Straneo F, Sutherland DA. 2014. Externally forced fluctuations in ocean temperature at Greenland glaciers in non-summer months. *Nat. Geosci.* 7:503–8

Jenkins A. 1991. A one dimensional model of ice-shelf ocean interaction. *J. Geophys. Res.* 96:20 671–77

Jenkins A. 1999. The impact of melting ice on ocean waters. *J. Phys. Oceanogr.* 29:2370–81

Jenkins A. 2011. Convection-driven melting near the grounding lines of ice shelves and tidewater glaciers. *J. Phys. Oceanogr.* 41:2279–94

Jenkins A, Nicholls KW, Corr HFJ. 2010. Observation and parameterization of ablation at the base of Ronne Ice Shelf, Antarctica. *J. Phys. Oceanogr.* 40:2298–312

Johnson HL, Münchow A, Falkner KK, Melling H. 2011. Ocean circulation and properties in Petermann Fjord, Greenland. *J. Geophys. Res.* 116:C01003

Joughin I, Smith BE, Shean DE, Floricioiu D. 2014. Brief communication: further summer speedup of Jakobshavn Isbræ. *Cryosphere* 8:209–14

Kader BA, Yaglom AM. 1972. Heat and mass transfer laws for fully turbulent wall flows. *Int. J. Heat Mass Transfer* 15:2329–51

Kimura S, Holland PR, Jenkins A, Piggott M. 2014. The effect of meltwater plumes on the melting of a vertical glacier face. *J. Phys. Oceanogr.* In press. doi: 10.1175/JPO-D-13-0219.1

Klinck JM, O'Brien JJ, Svendsen H. 1981. A simple model of fjord and coastal circulation interaction. *J. Phys. Oceanogr.* 11:1612–26

Lazier JRN. 1980. Oceanographic conditions at Ocean Weather Ship *Bravo*, 1964–1974. *Atmos.-Ocean* 18:227–38

Linden PF. 2000. Convection in the environment. In *Perspectives in Fluid Dynamics*, ed. GK Batchelor, HK Moffat, MG Worster, pp. 289–345. Cambridge, UK: Cambridge Univ. Press

Linden PF, Lane-Serff GF, Smeed DA. 1990. Emptying filling spaces: the fluid mechanics of natural ventilation. *J. Fluid Mech.* 212:300–35

Losch M. 2008. Modeling ice shelf cavities in a *z* coordinate ocean general circulation model. *J. Geophys. Res.* 113:C08043

MacCready P, Geyer WR. 2010. Advances in estuarine physics. *Annu. Rev. Mar. Sci.* 2:35–58
Mayer C, Reeh N, Jung-Rothenhäusler F, Huybrechts P, Oerter H. 2000. The subglacial cavity and implied dynamics under Nioghalvfjerdsfjorden Glacier, NE-Greenland. *Geophys. Res. Lett.* 27:2289–92
McPhee MG, Kottmeier C, Morison JH. 1999. Ocean heat flux in the central Weddell Sea during winter. *J. Phys. Oceanogr.* 29:1166–79
McPhee MG, Maykut GA, Morison JH. 1987. Dynamics and thermodynamics of the ice/upper ocean system in the marginal ice zone of the Greenland Sea. *J. Geophys. Res.* 92:7017–31
Mellor GL, McPhee MG, Steele M. 1986. Ice–seawater turbulent boundary layer interaction with melting and freezing. *J. Phys. Oceanogr.* 6:1829–46
Mortensen J, Bendtsen J, Motyka RJ, Lennert K, Truffer M, et al. 2013. On the seasonal freshwater stratification in the proximity of fast-flowing tidewater outlet glaciers in a sub-Arctic sill fjord. *J. Geophys. Res.* 118:1382–95
Mortensen J, Lennert K, Bendtsen J, Rysgaard S. 2011. Heat sources for glacial melt in a sub-Arctic fjord (Godthåbsfjord) in contact with the Greenland Ice Sheet. *J. Geophys. Res.* 116:C01013
Morton BR, Taylor GI, Turner JS. 1956. Turbulent gravitational convection from maintained and instantaneous sources. *Proc. R. Soc. A* 234:1–23
Motyka RJ, Hunter L, Echelmeyer KA, Connor C. 2003. Submarine melting at the terminus of a temperate tidewater glacier, LeConte Glacier, Alaska, USA. *Ann. Glaciol.* 36:57–65
Motyka RJ, Truffer M, Fahnestock M, Mortensen J, Rysgaard S, Howat I. 2011. Submarine melting of the 1985 Jakosbhavn Isbræ floating tongue and the triggering of the current retreat. *J. Geophys. Res.* 116:F01007
Münchow A, Padman L, Fricker HA. 2014. Interannual changes of the floating ice shelf of Petermann Gletscher, North Greenland, from 2000 to 2012. *J. Glaciol.* 60:489–99
Myers PG, Kulan N, Ribergaard MH. 2007. Irminger Water variability in the West Greenland Current. *Geophys. Res. Lett.* 34:L17601
Oltmanns M, Straneo F, Moore GWK, Mernild SH. 2014. Strong downslope wind events in Ammassalik, SE Greenland. *J. Clim.* 27:977–93
Rignot E, Koppes MC, Velicogna I. 2010. Rapid submarine melting of the calving faces of West Greenland glaciers. *Nat. Geosci.* 3:187–91
Schodlok MP, Menemenlis D, Rignot E, Studinger M. 2012. Sensitivity of the ice-shelf/ocean system to the sub-ice-shelf cavity shape measured by NASA IceBridge in Pine Island Glacier, West Antarctica. *Ann. Glaciol.* 53:156–62
Sciascia R, Cenedese C, Nicolì D, Heimbach P, Straneo F. 2014. Changes in submarine melting of a Greenland glacier induced by an intermediary circulation. *J. Geophys. Res.* In press
Sciascia R, Straneo F, Cenedese C, Heimbach P. 2013. Seasonal variability of submarine melt rate and circulation in an East Greenland fjord. *J. Geophys. Res.* 118:2492–506
Shepherd A, Ivins ER, Geruo A, Barletta VR, Bentley MJ, et al. 2012. A reconciled estimate of ice-sheet mass balance. *Science* 338:1183–89
Steele M, Mellor GL, McPhee MG. 1989. Role of the molecular sublayer in the melting or freezing of sea ice. *J. Phys. Oceanogr.* 19:139–47
Stigebrandt A. 1981. A mechanism governing the estuarine circulation in deep, strongly stratified fjords. *Estuar. Coast. Shelf Sci.* 13:197–211
Stigebrandt A. 1990. On the response of the horizontal mean vertical density distribution in a fjord to low-frequency density fluctuations in the coastal water. *Tellus* 42:605–14
Stigebrandt A. 2012. Hydrodynamic and circulations of fjords. In *Encyclopedia of Lakes and Reservoirs*, ed. L Bengtsson, RW Herschy, RW Fairbridge, pp. 327–44. Dordrecht, Neth.: Springer
Stigebrandt A, Aure J. 1990. *The importance of external driving forces for the water exchange in the fjords from Skagerrak to Finnmark*. Rep. FO9003, Inst. Mar. Res., Bergen, Nor. (in Norwegian)
Stommel H, Farmer HG. 1953. Control of salinity in an estuary by a transition. *J. Mar. Res.* 12:13–20
Straneo F, Curry RG, Sutherland DA, Hamilton GS, Cenedese C, et al. 2011. Impact of fjord dynamics and glacial runoff on the circulation near Helheim Glacier. *Nat. Geosci.* 4:322–27
Straneo F, Hamilton GS, Sutherland DA, Stearns LA, Davidson F, et al. 2010. Rapid circulation of warm subtropical waters in a major glacial fjord in East Greenland. *Nat. Geosci.* 3:182–86

Straneo F, Heimbach P. 2013. North Atlantic warming and the retreat of Greenland's outlet glaciers. *Nature* 504:36–43

Straneo F, Heimbach P, Sergienko O, Hamilton G, Catania G, et al. 2013. Challenges to understand the dynamic response of Greenland's marine terminating glaciers to oceanic and atmospheric forcing. *Bull. Am. Meteorol. Soc.* 94:1131–44

Straneo F, Sutherland DA, Holland D, Gladish C, Hamilton GS, et al. 2012. Characteristics of ocean waters reaching Greenland's glaciers. *Ann. Glaciol.* 53:202–10

Sutherland DA, Pickart RS. 2008. The East Greenland Coastal Current: structure, variability, and forcing. *Prog. Oceanogr.* 78:58–77

Sutherland DA, Straneo F. 2012. Estimating ocean heat transports and submarine melt rates in Sermilik Fjord, Greenland, using lowered acoustic Doppler current profiler (LADCP) velocity profiles. *Ann. Glaciol.* 53:50–58

Sutherland DA, Straneo F, Pickart RS. 2014. Characteristics and dynamics of two major Greenland glacial fjords. *J. Geophys. Res.* 119:3767–91

Svendsen H. 1980. Exchange processes above sill level between fjords and coastal water. In *Fjord Oceanography*, ed. HJ Freeland, DM Farmer, CD Levings, pp. 355–62. New York: Plenum

Syvitski JPM. 1989. On the deposition of sediment within glacier-influenced fjords: oceanographic controls. *Mar. Geol.* 85:301–29

Taylor GI. 1958. Flow induced by jets. *J. Aerosp. Sci.* 25:464–65

Turner JS. 1979. *Buoyancy Effects in Fluids*. New York: Cambridge Univ. Press. 2nd ed.

van den Broeke M, Bamber J, Ettema J, Rignot E, Schrama E, et al. 2009. Partitioning recent Greenland mass loss. *Science* 326:984–86

Vieli A, Nick FM. 2011. Understanding and modelling rapid dynamic changes of tidewater outlet glaciers: issues and implications. *Surv. Geophys.* 32:437–58

Xu Y, Rignot E, Fenty I, Menemenlis D, Flexas MM. 2013. Subaqueous melting of Store Glacier, west Greenland from three-dimensional, high-resolution numerical modeling and ocean observations. *Geophys. Res. Lett.* 40:4648–53

Xu Y, Rignot E, Menemenlis D, Koppes M. 2012. Numerical experiments on subaqueous melting of Greenland tidewater glaciers in response to ocean warming and enhanced subglacial discharge. *Ann. Glaciol.* 53:229–34

Annual Review of
Marine Science

Volume 7, 2015

Contents

Errata

An online log of corrections to *Annual Review of Marine Science* articles may be found at http://www.annualreviews.org/errata/marine